DALTON

Crystallographic, vibrational and nuclear magnetic resonance spectroscopic characterization of the $[(PhS)_2Hg(\mu\text{-}SPh)_2Hg(SPh)_2]^{2-}$ ion

Graham A. Bowmaker,*[a] Ian G. Dance,[b] Robin K. Harris,[c] William Henderson,[d] Ian Laban,[a] Marcia L. Scudder[b] and Se-Woung Oh[c]

[a] *Department of Chemistry, University of Auckland, Private Bag 92019, Auckland, New Zealand*
[b] *School of Chemistry, University of New South Wales, PO Box 1, Kensington, NSW 2033, Australia*
[c] *Department of Chemistry, University of Durham, South Rd., Durham DH1 3LE, UK*
[d] *Department of Chemistry, University of Waikato, Private Bag 3105, Hamilton, New Zealand*

The complex $[NMe_4]_2[Hg_2(SPh)_6]$ has been prepared and characterized by X-ray crystallography, vibrational and solid-state NMR spectroscopy. It contains the bitetrahedral $[(PhS)_2Hg(\mu\text{-}SPh)_2Hg(SPh)_2]^{2-}$ anion, in contrast to the $[NBu^n_4]^+$ salt of the same stoichiometry, which contains the distorted-trigonal $[Hg(SPh)_3]^-$ species. The structures of these two species are related in the sense that they both contain relatively strongly bound $Hg(SPh)_2$ units with weaker bonding to the additional PhS^- ligand(s). This relationship is reflected in the ^{199}Hg magic angle spinning NMR spectra through similarities in the chemical shift parameters, and in the far-IR and Raman spectra through similarities in the ν(HgS) vibrational frequencies. Solution ^{199}Hg NMR and electrospray mass spectra of $[NMe_4]_2[Hg_2(SPh)_6]$ indicate that $[Hg_2(SPh)_6]^{2-}$ dissociates readily into $[Hg(SPh)_3]^-$ in solution, confirming the relative weakness of the bridge bonding in the dinuclear complex.

The great affinity of thiols for mercury has been known for a long time, and is the basis of the name 'mercaptan' for this class of compound. Thiolate ligands play an important role in the biological chemistry of the Group 12 metals, and the co-ordination of cysteine residues of metallothioneins and of metalloregulatory proteins to zinc, cadmium[1,2] and mercury[3-6] is of particular relevance in this connection. Thiolate complexes of the divalent Group 12 metals show a considerable degree of variation in their co-ordination geometry: tetrahedral four-co-ordination predominates for zinc and cadmium, whereas linear two-co-ordination and trigonal three-co-ordination are also important for mercury.[7,8] All three of the above geometries have been proposed for mercury(II) in biological systems.[4,6,9] The factors which determine the different co-ordination geometries are not clear. Even for the case of homoleptic complexes of the type $[Hg(SR)_n]^{2-n}$ the range of structural types is considerable. For bis(thiolato)mercury(II) complexes of general formula $Hg(SR)_2$ both linearly co-ordinated monomeric[3,8-16] and distorted tetrahedrally co-ordinated polymeric[16-19] structures have been found, and there is no clear relationship between the nature of the substituent R and the structure type.

Several tris(thiolato)mercurate complexes have been investigated by X-ray crystallography, and all but one are mononuclear $[Hg(SR)_3]^-$ with trigonal-planar or distorted trigonal-planar co-ordination.[3,5,19-21] The one exception to date is the dinuclear doubly bridged structure observed for the $[Hg_2(SMe)_6]^{2-}$ anion in its tetraethylammonium salt, although this ion was shown by Raman spectroscopy to dissociate in solution to give mononuclear $[Hg(SMe)_3]^-$ ions.[22] In contrast to the situation for mercury(II) complexes, zinc(II) and cadmium(II) thiolate complexes of 1 : 3 stoichiometry show a strong preference for the dinuclear $[M_2(SR)_6]^{2-}$ structure.[23,24] The fact that the reported structures of the benzenethiolate complexes of the Group 12 metals show the mononuclear $[M(SPh)_3]^-$ structure for M = Hg,[20] but the dinuclear $[M_2(SPh)_6]^{2-}$ structure for M = Zn or Cd,[23] has been quoted as a good illustration of this point.[19]

Thiolate ligands have pseudo-halide characteristics,[7,25,26] and the structural chemistry described in the previous paragraph has parallels in that of the corresponding halogeno-complexes. However, the observation of trigonal-planar $[HgX_3]^-$ in the solid state is rather rare, in contrast to the situation for the corresponding thiolate complexes. Most frequently the dinuclear doubly halide-bridged $[Hg_2X_6]^{2-}$ ions are observed in the solid state,[27-29] although the mononuclear $[HgX_3]^-$ species is readily identified by Raman spectroscopy in solution.[30] One of the factors which determines whether $[HgX_3]^-$ or $[Hg_2X_6]^{2-}$ is formed in the solid state is the nature of the associated cation. Thus, $[NBu^n_4][HgI_3]$ is one of the few examples of a compound which contains discrete mononuclear $[HgX_3]^-$ in the solid state, but the corresponding complex with $[NPr^n_4]^+$ rather than $[NBu^n_4]^+$ as the cation contains the dinuclear doubly halide-bridged $[Hg_2I_6]^{2-}$ anion.[27] Thus, an increase in the size of the cation results in the isolation of the mononuclear anion. Since the previously reported compound which contains mononuclear $[Hg(SPh)_3]^-$ involves the relatively large cation $[NBu^n_4]^+$,[20] it seemed likely that the analogous complexes with smaller cations would contain the hitherto unreported $[Hg_2(SPh)_6]^{2-}$ species. This proved to be the case for the tetramethylammonium compound $[NMe_4]_2[Hg_2(SPh)_6]$ of which the preparation, crystal structure and characterization by vibrational and solid-state NMR spectroscopy are reported in the present work.

Experimental

Preparations

All reactions were carried out in Schlenk tubes under an atmosphere of oxygen-free nitrogen.

Bis(tetramethylammonium)bis(μ-benzenethiolato)tetrakis(benzenethiolato)dimercurate(II), $[NMe_4]_2[Hg_2(SPh)_6]$. Benzenethiol (3.31 g, 30 mmol) was added to mercury(II) oxide (2.2 g, 10 mmol) suspended in ethanol (5 cm^3). Tetramethylammonium hydroxide (3.65 g of a 25% solution in water; contains 0.91 g, 10 mmol) was added to this mixture and the benzenethiol and tetramethylammonium hydroxide containers were each rinsed with ethanol (5 cm^3) which was then added to the reaction mixture. The mixture was heated to about 90 °C and

stirred for 1.25 h, after which time most of the solid material had dissolved. Upon cooling to room temperature an oil separated, and this solidified upon further cooling to 0 °C. The supernatant liquid was decanted off, and the solid redissolved in ethanol (100 cm^3) at 90 °C. The solution was filtered while hot, and a large amount of white cloudy oil separated from the filtrate upon cooling. More ethanol (20 cm^3) was added and the mixture heated until a clear yellow solution was obtained. At first an oil separated again upon cooling, but this quickly solidified, and the remainder of the product separated upon further cooling as a white crystalline solid. Yield 4.66 g (78%). M.p. 116–119 °C (Found: C, 44.6; H, 5.2. Calc. for $C_{44}H_{54}Hg_2N_2S_6$: C, 43.9; H, 4.5%). The compound is soluble in protic solvents (*e.g.* ethanol), strong dipolar aprotic solvents (*e.g.* acetonitrile, Me_2SO) but not in weakly polar solvents (*e.g.* chloroform).

Tetra-*n*-butylammonium tris(benzenethiolato)mercurate(II), $[NBu^n_4][Hg(SPh)_3]$. This was prepared by reaction of NaSPh, HgO and $[NBu^n_4]Br$ in a 5:1:2 ratio in methanol, in a modification of the literature method.[20] M.p. 125–127 °C.

X-Ray crystallography

Diffraction data for $[NMe_4]_2[Hg_2(SPh)_6]$ were measured on an Enraf-Nonius CAD-4 diffractometer in 2θ–θ scan mode using graphite-monochromated molybdenum radiation (λ 0.7107 Å) yielding 8287 independent reflections, 5053 with $I > 3\sigma(I)$ being considered 'observed'. The methods used for data processing and reduction have been described.[31] Data were corrected for absorption using numerical integration over a 6 × 6 × 6 Gaussian grid. The structure of the anion was determined by a combination of Patterson and Fourier methods. The $[NMe_4]^+$ groups were poorly defined and so were refined as rigid groups of perfect tetrahedral geometry.[32] One variable was used to refine a global N–C distance. The thermal motion of each cation was described as a 15-parameter TLX group (where T is the translation vector, L the libration vector and X the origin of libration). The atoms of the anion were refined individually with anisotropic thermal parameters. Hydrogen atoms were included in calculated positions and assigned thermal parameters equal to those of the atom to which they were bonded. Reflection weights used were $1/\sigma^2(F_o)$ with $\sigma(F_o)$ being derived from $\sigma(I_o) = [\sigma^2(I_o) + (0.04I_o)^2]^{\frac{1}{2}}$. The weighted residual is defined as $R' = (\Sigma w\Delta^2/\Sigma wF_o^2)^{\frac{1}{2}}$. Atomic scattering factors and anomalous dispersion parameters were obtained from published tables.[33] The program ORTEP II[34] running on a Macintosh IIcx computer was used for the structure diagram, and an IBM 3090 computer was used for the calculations.

Crystal/refinement data. $[NMe_4]_2[Hg_2(SPh)_6]$, $C_{44}H_{54}Hg_2N_2S_6$, $M = 1204.6$, monoclinic, space group $P2_1/c$, $a = 19.84(1)$, $b = 15.666(3)$, $c = 16.284(9)$ Å, $\beta = 110.91(3)°$, $U = 4728(4)$ Å^3, $Z = 4$, $D_c = 1.69$ g cm^{-3}, $F(000) = 2352$, $\mu = 67.7$ cm^{-1}, specimen 0.46 × 0.30 × 0.28 mm, $A^*_{min,max} = 0.20, 0.11$, $2\theta_{max} = 50°$, $T = 21$ °C, $R = 0.035$, $R' = 0.042$.

Atomic coordinates, thermal parameters, and bond lengths and angles have been deposited at the Cambridge Crystallographic Data Centre (CCDC). See Instructions for Authors, *J. Chem. Soc., Dalton Trans.*, 1996, Issue 1. Any request to the CCDC for this material should quote the full literature citation and the reference number 186/43.

Spectroscopy

Far-infrared spectra were recorded at 2 cm^{-1} resolution at room temperature as pressed Polythene discs using a Digilab FTS-60 Fourier-transform spectrometer employing an FTS-60V vacuum optical bench with a 6.25 μm mylar-film beam splitter, a mercury-lamp source and a pyroelectric triglycine sulfate detector. Raman spectra were recorded at 4.5 cm^{-1} resolution using a Jobin-Yvon U1000 spectrometer equipped with a cooled photomultiplier (RCA C31034A) detector. The 488.0 nm exciting line from a Spectra-Physics model 2016 argon-ion laser was used. Carbon-13 and mercury-199 magic-angle spinning spectra were obtained at 75.43 and 53.68 MHz, respectively, using a Varian Unity Plus 300 spectrometer. A sapphire rotor (outside diameter 7.0 mm) with Kel-F end-caps was employed for the ^{13}C spectra, with spin rates in the range 4–5 kHz, whereas a silicon nitride rotor (outside diameter 5.0 mm) with Vespel end-caps was necessary for the ^{199}Hg spectra in order to reach spin rates in the range 11–13 kHz (resulting in a minimum number of spinning sidebands). Although measurements were nominally made at ambient probe temperature (*ca.* 25 °C), it is likely that the fast spinning used for the ^{199}Hg spectra resulted in substantially elevated temperatures (*ca.* 45 °C).[35] For both nuclei high-power proton decoupling (equivalent to 60 kHz) was used. Cross-polarization (with flip-back) was employed for ^{13}C spectra, with variation of contact times explored over the range 0.2–20 ms. Optimum contact times for the quaternary, aromatic CH and NMe_4 carbons were *ca.* 2.0, 0.5 and 5 ms respectively, reflecting the variation of characteristic cross-polarization times $T_{cp} \approx 0.6, 0.1$ and 5.8 ms respectively. Values of $T_{1\rho}(^1H)$ derived from the variable-contact time experiment were 4.5, 5.6 and 9.1 ms respectively, the first two being equal within experimental error (though the result for the NMe_4 group may reflect incomplete spin diffusion). For the ^{13}C spectra recycle delays of 10 s were optimum and 60–100 transients gave good-quality spectra. Mercury-199 spectra were recorded with direct polarization {4.5 μs 90° pulses as judged *via* cross polarization for a sample of $[Hg(dmso)_6][O_3SCF_3]_2$ (dmso = dimethyl sulfoxide)}. Centreband signals were located by varying the spinning rate. Recycle delays of 60 s were necessary with *ca.* 1000 transients necessary to get acceptable spectra. Spinning sideband intensities were analysed to yield values of the shielding-tensor components by an iterative computer program written in-house.[36] The fitting procedure used a total of five sidebands plus the centreband, and was carried out for a spinning speed of 11.0 kHz. Accuracy was limited by the high noise level, and because the spectrum required baseline correction. Chemical shifts were referenced using replacement samples of adamantane (δ_C 38.4 for the CH_2 carbon on the tetramethylsilane scale) and $[Hg(dmso)_6][O_3SCF_3]_2$ (δ_{Hg} −2313[37] on the dimethylmercury scale). Solution mercury-199 NMR spectra were obtained at 71.64 MHz at ambient probe temperature using a Bruker DRX 400 MHz spectrometer and processed using Bruker UXNMR (Version 941001.2) software running on a Silicon Graphics workstation. The sample was measured in a 10 mm NMR tube using 20 μs 90° pulses. Chemical shifts were referenced to $HgMe_2$ *via* 0.5 mol dm^{-3} HgPh(Cl) in dmso (δ_{Hg} −1186.6[38] on the dimethylmercury scale). Electrospray mass spectra were obtained in negative-ion mode with a VG Platform II mass spectrometer using acetonitrile–water (1:1 v/v) as mobile phase. The compound was dissolved in the mobile phase to give a solution typically of approximate concentration 0.1 mmol dm^{-3}, and spectra were recorded on the freshly prepared solutions. The diluted solution was injected into the spectrometer *via* a Rheodyne injector fitted with a 10 μl sample loop. A Thermo Separation Products SpectraSystem P1000 LC pump delivered the solution to the mass spectrometer source (60 °C) at a flow rate of 0.01 cm^3 min^{-1}, and nitrogen was employed both as drying and nebulizing gas. Cone voltages were varied from 5 to 60 V in order to investigate the effect of higher voltages on the fragmentation of parent ions. Confirmation of the species detected is aided by comparison of the observed and predicted isotope distribution patterns. Theoretical isotope distribution patterns were calculated using the ISOTOPE computer program.[39]

Results and Discussion

Structure of $[NMe_4]_2[Hg_2(SPh)_6]$

The asymmetric unit in the crystal structure consists of one formula unit, *i.e.* $[Hg_2(SPh)_6]^{2-}$ and two $[NMe_4]^+$ ions. The structure of the bitetrahedral $[(PhS)_2Hg(\mu\text{-}SPh)_2Hg(SPh)_2]^{2-}$ anion is shown in Fig. 1, and the core geometry parameters are compared with those of the corresponding methanethiolate complex in Table 1. Despite the lower symmetry of the benzenethiolate complex, which lacks the centre of symmetry present in the methanethiolate,[22] the structural parameters for both compounds are remarkably similar. In both cases the expected shortening of the terminal relative to the bridging Hg–S bonds is observed, although this effect is slightly more pronounced in the benzenethiolate complex. Similar distortions of the mercury co-ordination environments from ideal tetrahedral geometry are observed in both cases. Thus the S–Hg–S angle involving the bridging S atoms [89.9(1)°] is significantly less than the ideal tetrahedral angle (109.5°), while that involving the terminal S atoms is considerably greater at 132.4(1)°. Again, this effect is more pronounced in the benzenethiolate complex, particularly in respect of the S–Hg–S angle involving the terminal S atoms, the value for the benzenethiolate complex being *ca.* 10° greater than that for the methanethiolate. This is probably related to the presence of shorter terminal Hg–S bonds (see above), both of these observations being a consequence of stronger terminal Hg–S bonding in the present complex.

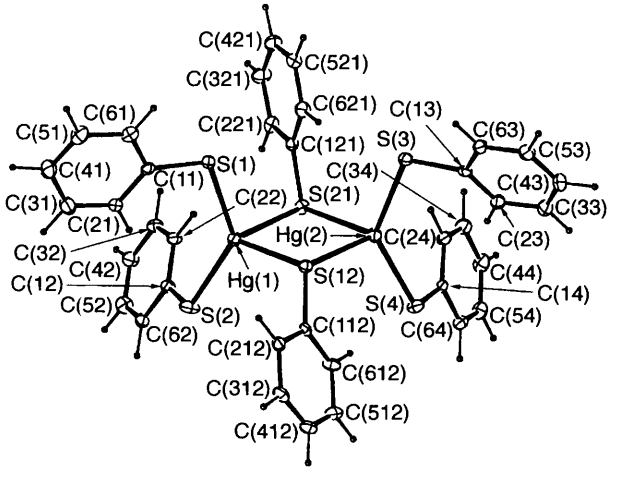

Fig. 1 Structure of the $[Hg_2(SPh)_6]^{2-}$ ion in $[NMe_4]_2[Hg_2(SPh)_6]$

Table 1 Comparison of selected bond lengths (Å) and angles (°) for the anions in $[NMe_4]_2[Hg_2(SPh)_6]$ and $[NEt_4]_2[Hg_2(SMe)_6]$

$[NMe_4]_2[Hg_2(SPh)_6]$		$[NEt_4]_2[Hg_2(SMe)_6]$*	
Hg(1)–S(12)	2.645(2)	Hg–S(1)	2.629(2)
Hg(2)–S(12)	2.695(2)		
Hg(1)–S(21)	2.707(2)	Hg–S(1′)	2.706(2)
Hg(2)–S(21)	2.696(2)		
Hg(1)–S(1)	2.442(2)	Hg–S(2)	2.473(2)
Hg(2)–S(3)	2.439(2)		
Hg(1)–S(2)	2.426(2)	Hg–S(3)	2.438(2)
Hg(2)–S(4)	2.440(2)		
S(12)–Hg(1)–S(21)	89.9(1)	S(1)–Hg–S(1′)	94.27(5)
S(12)–Hg(2)–S(21)	89.1(1)		
S(12)–Hg(1)–S(1)	100.9(1)	S(1)–Hg–S(2)	106.98(6)
S(12)–Hg(2)–S(3)	103.8(1)		
S(12)–Hg(1)–S(2)	114.4(1)	S(1)–Hg–S(3)	116.09(7)
S(12)–Hg(2)–S(4)	109.1(1)		
S(21)–Hg(1)–S(1)	102.0(1)	S(1′)–Hg–S(2)	104.94(6)
S(21)–Hg(2)–S(3)	106.1(1)		
S(21)–Hg(1)–S(2)	108.6(1)	S(1′)–Hg–S(3)	108.68(7)
S(21)–Hg(2)–S(4)	107.8(1)		
S(1)–Hg(1)–S(2)	132.4(1)	S(2)–Hg–S(3)	121.87(7)
S(3)–Hg(2)–S(4)	132.4(1)		
Hg(1)–S(12)–Hg(2)	91.2(1)	Hg–S(1)–Hg′	85.73(5)
Hg(1)–S(21)–Hg(2)	89.8(1)		

* Ref. 22.

IR and Raman spectroscopy

The far-IR and Raman spectra of $[NMe_4]_2[Hg_2(SPh)_6]$ and $[NBu^n_4][Hg(SPh)_3]$ are shown in Figs. 2 and 3. In a previous study of some cyclohexanethiolate complexes of mercury(II) a correlation was developed between the co-ordination geometry, the Hg–S bond lengths, and the Hg–S stretching frequencies ν(HgS) of these and a number of other homoleptic thiolate complexes of mercury.[19] This correlation did not include any examples of benzenethiolate complexes, however. The present results allow an investigation of the validity of this correlation for complexes of benzenethiolate, which is one of the most common thiolate ligands used in co-ordination chemistry. A potential complication arises in this case because this ligand has internal vibrations which appear to be very sensitive to the mode of co-ordination, probably due to coupling of the ν(HgS) modes to the internal ligand modes concerned.[40] Nevertheless, it is possible to make ν(HgS) assignments which are consistent with those reported previously for other mercury(II) thiolate compounds.[19,22]

We consider first the far-IR spectrum of $[NMe_4]_2[Hg_2(SPh)_6]$ [Fig. 2(*a*)]. Since the terminal Hg–S bonds are significantly shorter than the bridging bonds in this compound

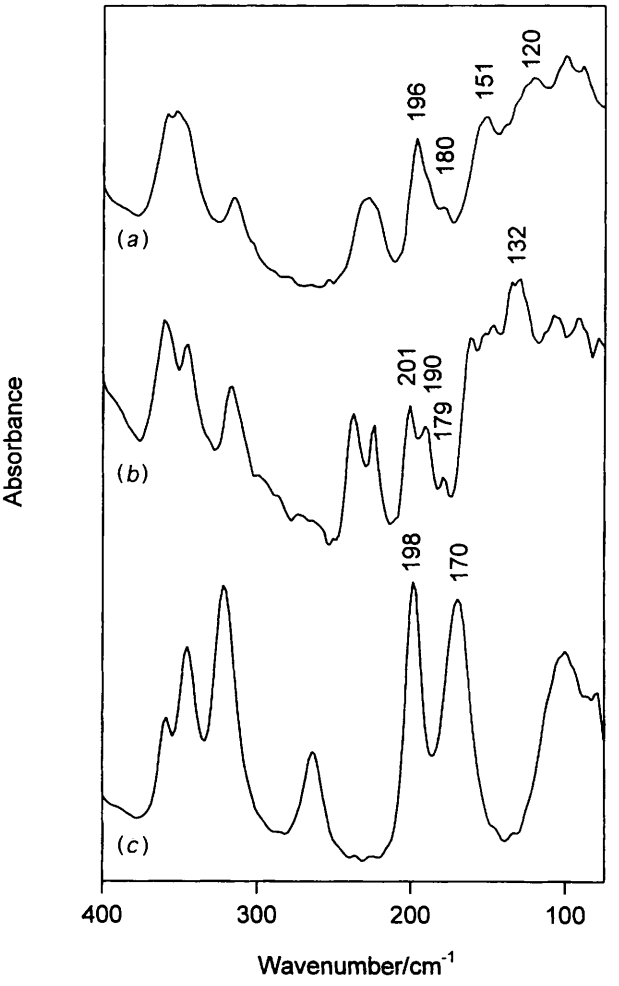

Fig. 2 Far-IR spectra of (*a*) $[NMe_4]_2[Hg_2(SPh)_6]$, (*b*) $[NMe_4]_2[Hg_2(SPh)_6]$ at low temperature (*ca.* 120 K), and (*c*) $[NBu^n_4][Hg(SPh)_3]$. Bands assigned as ν(HgS) are labelled with their wavenumbers

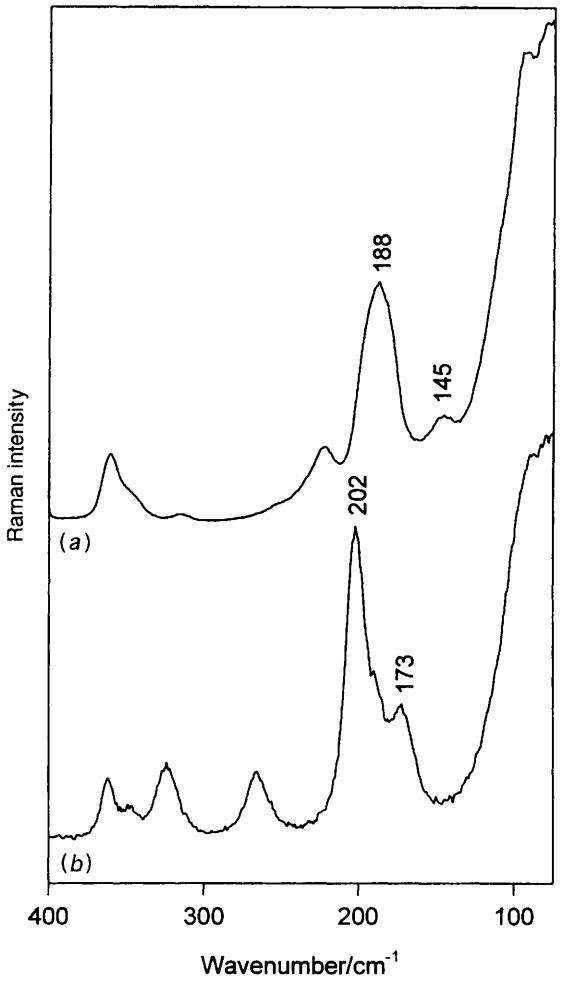

Fig. 3 Raman spectra of (*a*) $[NMe_4]_2[Hg_2(SPh)_6]$ and (*b*) $[NBu^n_4][Hg(SPh)_3]$. Bands assigned as ν(HgS) are labelled with their wavenumbers

the terminal ν(HgS) modes are expected to be higher in wavenumber than the bridging modes, as was the case for the corresponding methanethiolate complex.[22] In that case the terminal ν(HgS) modes occur at about 270 cm^{-1}, and it was found that the terminal ν(HgS) wavenumber was sensitive to the nature of the thiolate ligand, decreasing to 208 cm^{-1} for $[Hg(SBu^t)_3]^-$. The main reason for this decrease appears to be the increase in the mass of the thiolate ligand; the ratio of the observed wavenumbers is close to the square root of the inverse of the masses of the thiolate ligands concerned. Since PhS^- has a greater mass than Bu^tS^- the wavenumbers in the present complex should lie below 200 cm^{-1}. Thus we assign the IR bands at 196, 180 (IR) and 188 cm^{-1} (Raman) to the terminal ν(HgS) modes. The bands at 151, 120 (IR) and 145 cm^{-1} (Raman) are assigned to the bridging ν(HgS) modes. These assignments are supported by the fact that the relative intensities of the terminal and bridging bands behave in a similar way to those of the simpler $[Hg_2(SMe)_6]^{2-}$ and $[Hg_2Cl_6]^{2-}$ complexes.[22,27] Thus the terminal modes are of comparable intensity to the bridging modes in the IR spectrum, but are much stronger in the Raman spectrum. In particular, the fact that the Raman band at 188 cm^{-1} of $[Hg_2(SPh)_6]^{2-}$ is considerably more intense than the neighbouring bands in this region is strong support for the assignment of this band to the terminal ν(HgS) mode.

The far-IR spectrum of $[NBu^n_4][Hg(SPh)_3]$ shows two bands in the ν(HgS) region at 198, 170 cm^{-1} [Fig. 2(*c*)]. The structure of the $[Hg(SPh)_3]^-$ species in this complex is strongly distorted from ideal trigonal-planar HgS_3 geometry. The distortion is such that one of the S–Hg–S angles [137.1(1)°], is

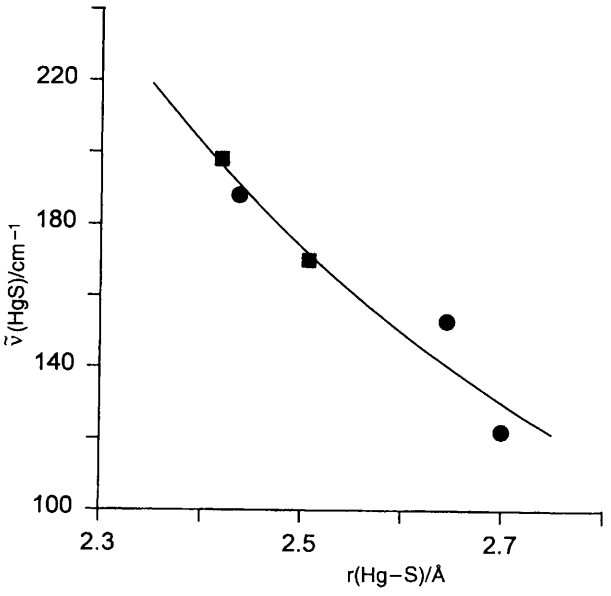

Fig. 4 Plot of the wavenumber of the ν(HgS) IR band *vs.* the Hg–S bond length in $[NMe_4]_2[Hg_2(SPh)_6]$ (●) and $[NBu^n_4][Hg(SPh)_3]$ (■)

significantly greater than the trigonal angle of 120°, and the two Hg–S bonds which form this angle are significantly shorter [2.407(3), 2.431(3) Å] than the third [2.507(3)°]. The symmetry of the local HgS_3 array is thus reduced from D_{3h} (for ideal trigonal-planar geometry) to C_s and the IR-active ν(HgS) mode of E symmetry under D_{3h} is expected to split into two bands for the distorted complex, and this agrees with the experimental result. Since the IR-active vibration involving the two shorter Hg–S bonds is expected to be approximately orthogonal to and therefore not strongly coupled to that of the longer bond, an alternative interpretation is that the band at 198 cm^{-1} is due to the shorter bonds and that at 170 cm^{-1} to the longer bond. Corresponding bands are observed in the Raman spectrum [Fig. 3(*b*)] at 202 and 173 cm^{-1} respectively. This interpretation fits well with that discussed above for $[NMe_4]_2[Hg_2(SPh)_6]$. Fig. 4 shows a plot of the wavenumbers of the ν(HgS) IR bands for both compounds against the Hg–S bond lengths. The average of the two shorter bond lengths has been used for the band at 198 cm^{-1} of $[NBu^n_4][Hg(SPh)_3]$, while the average of the four terminal Hg–S bond lengths and the two terminal ν(HgS) wavenumbers has been used for $[NMe_4]_2[Hg_2(SPh)_6]$. For the bridging bonds in this compound it can be noted that one of the bond lengths [2.645(2) Å] is considerably shorter than the other three [average 2.699(5) Å], and the bands at 151, 120 cm^{-1} have been assigned accordingly. The data in Fig. 4 show a monotonic variation of wavenumber with bond length, although the points for the bridging bonds in $[NMe_4]_2[Hg_2(SPh)_6]$ show a considerably greater deviation from the best-fit curve than do those for the terminal bonds. For these bridging bonds there is also a significantly greater difference between the IR and the Raman wavenumbers, indicating that mechanical coupling of the vibrations of the individual bonds is more important here than for the terminal bonds. However, the overall correlation is reasonable, suggesting that the assignments made here are reasonably consistent. The resolution of the bands in the far-IR spectrum of $[NMe_4]_2[Hg_2(SPh)_6]$ is significantly improved at lower temperature [Fig. 2(*b*)], and in this spectrum the strongest band in the bridging ν(HgS) region occurs at about 132 cm^{-1}, which is exactly the wavenumber predicted by the correlation in Fig. 4 for the three longer bridging Hg–S bonds of length *ca.* 2.7 Å. The only other benzenethiolatomercurate(II) compound for which vibrational spectra have been reported is $[PPh_4][Hg(SPh)_3]$, for which the assignments ν(HgS) 178, 158 (IR), 180 cm^{-1} (Raman) were

Table 2 Magic angle spining ^{199}Hg NMR parameters[a] for $[NMe_4]_2[Hg_2(SPh)_6]$ and some related compounds

Compound	Co-ordination number[b]	σ_{11}	σ_{22}	σ_{33}	$\Delta\sigma$	δ_{iso}	η	Ref.
$[NMe_4]_2[Hg_2(SPh)_6]$	4	−105	444	1315	1145	−551	0.72	*c*
		−92	453	1359	1178	−574	0.69	*c*
$[NEt_4]_2[Hg(SC_6H_4Ph\text{-}2)_4]$	4	379	429	491	87	−433	0.86	*d*
$[NBu^n_4][Hg(SPh)_3]$	3	−494	326	1190	1273	−341	0.97	*d*
$[PPh_4][Hg(SC_6H_2Pr^i_3\text{-}2,4,6)_3]$	3	876	596	−672	−1408	−267	0.30	*d*
$[NMe_4][Hg(SPr^i)_3]$	3	433	433	−629	−1062	−79	0.00	*e*
$[Hg(SC_6H_2Pr^i_3\text{-}2,4,6)_2]$	2	−627	−180	3852	4256	−1015	0.16	*d*

[a] $\Delta\sigma = \sigma_{33} - (\sigma_{11} + \sigma_{22})/2$; $\delta_{iso} = -\sigma_{iso} = -(\sigma_{11} + \sigma_{22} + \sigma_{33})/3$; $\eta = (\sigma_{22} - \sigma_{11})/(\sigma_{33} - \sigma_{iso})$; the principal components σ_{11}, σ_{22}, σ_{33} of the shielding tensor are defined such that $|\sigma_{33} - \sigma_{iso}| \geq |\sigma_{11} - \sigma_{iso}| \geq |\sigma_{22} - \sigma_{iso}|$. [b] Of mercury. [c] This work; estimated accuracy of σ_{11}, σ_{22}, σ_{33}, $\Delta\sigma$ is ± 30 ppm, of η is ± 0.08. [d] Ref. 21; the signs of σ_{11}, σ_{22} and σ_{33} have been reversed to give values which are consistent with the definition of σ as a shielding parameter. [e] Calculated from the spectrum (spinning speed 4 kHz) given in ref. 44.

made.[41] A mononuclear structure for the anion was assumed, and the presence of two bands was interpreted in terms of a trigonal-pyramidal rather than a trigonal-planar HgS_3 geometry. In view of the more recently published structure of $[NBu^n_4][Hg(SPh)_3]$,[20] the possibility that it contains a distorted trigonal-planar species should also be considered. However, the reported wavenumbers are significantly lower than those found in the present study for the $[NBu^n_4]^+$ compound, and are actually closer to those for the dinuclear complex in $[NMe_4]_2[Hg_2(SPh)_6]$. This suggests that the $[PPh_4]^+$ compound also contains the dinuclear anion, and this has been verified by a crystal structure determination. This is contrary to the generalization mentioned in the Introduction, namely that an increase in the size of the cation should favour the mononuclear anion over the dimer. However, supramolecular interactions are influential in crystal structures, and in particular the sextuple phenyl embrace (concert of six attractive edge-to-face interactions between phenyl groups) between $[PPh_4]^+$ cations[42] is a dominant feature, probably more important than ion size. We will analyse the crystal supramolecularity in these compounds in a subsequent paper.

Solid-state NMR spectroscopy

It has recently been shown that MAS ^{199}Hg NMR spectroscopy is a powerful method for distinguishing different co-ordination environments in mercury thiolate complexes.[21,43,44] The environments examined in these studies were two-, three- and four-co-ordinate, but in the last-mentioned case the four thiolate ligands were either all terminal, as in $[Hg(SR)_4]^{2-}$, or all bridging, as in the chain-polymer structure of $[Hg(SBu^t)_2]$. No results were reported for complexes containing a mixture of terminal and bridging ligands, so the results for the $[Hg_2(SPh)_6]^{2-}$ complex obtained in the present study represent the first data on this type of co-ordination environment.

The MAS ^{199}Hg NMR spectrum of $[NMe_4]_2[Hg_2(SPh)_6]$ is shown in Fig. 5. As with other mercury complexes which show large shielding anisotropy, the spectrum consists of a centreband flanked by a number of spinning sidebands.[21,43,45] The centreband is a doublet (δ_{Hg} −551 and −574), as is each of the sidebands as a result of the presence of two inequivalent Hg atoms, and this is entirely consistent with the crystal structure which shows that the two Hg atoms in the dimer are crystallographically inequivalent (see above). The ^{199}Hg chemical shift parameters derived from this spectrum are compared in Table 2 with those for a number of other mercury(II) thiolate compounds with different co-ordination environments. The parameters for the two inequivalent sites are probably equal within experimental error, in agreement with the crystal-structure data, which show that the environments for Hg(1) and Hg(2) are very similar (Table 1). The shielding anisotropy $\Delta\sigma$ is much greater than that in

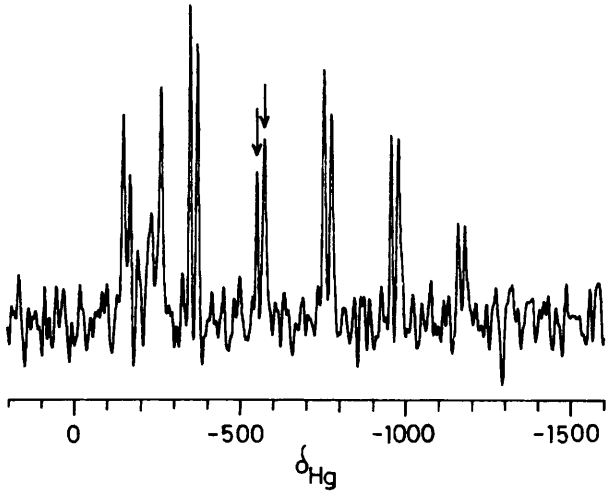

Fig. 5 The 53.68 MHz ^{199}Hg MAS NMR spectrum of $[NMe_4]_2[Hg_2(SPh)_6]$, showing the pair of centrebands (arrowed) and associated spinning sidebands. 2016 Points were acquired in the free induction decay, which was filled to 64 k before Fourier transformation. Gaussian broadening equivalent to 0.0012 s was employed for the plot

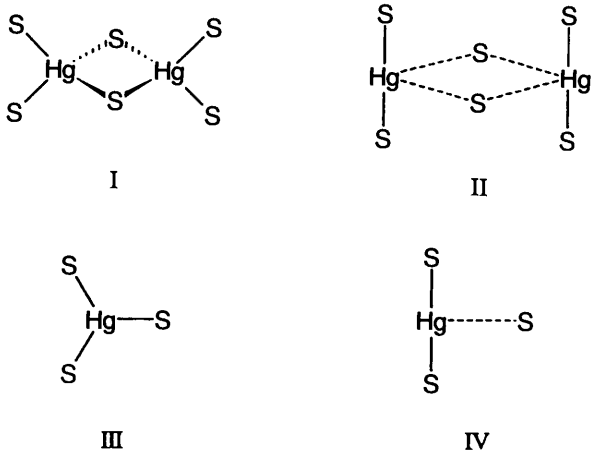

$[NEt_4][Hg(SC_6H_4Ph\text{-}2)_4]$ in which all four thiolate ligands are terminal. This, too, is in accord with the structural data which show that the two terminal bonds are significantly stronger than the two bridging bonds at each of the Hg atoms, and that the angular distortions from tetrahedral geometry are such that the structure of the complex can be regarded as being intermediate between one involving ideal tetrahedral co-ordination at the two Hg atoms (**I**) and one which can be described as two linearly co-ordinated $Hg(SPh)_2$ molecules connected by two bridging PhS^- ligands (**II**). A similar

situation obtains in $[NBu^n_4][Hg(SPh)_3]$, where the distorted trigonal-planar structure of the $[Hg(SPh)_3]^-$ ion can be regarded as intermediate between ideal trigonal planar (**III**) and one which can be described as a linearly co-ordinated $Hg(SPh)_2$ molecule with an additional weakly bound PhS^- ligand (**IV**).

It is therefore of interest that the shielding anisotropy $\Delta\sigma$ in the present four-co-ordinate complex has a value which is much closer to that for the three-co-ordinate $[Hg(SPh)_3]^-$ than to that for the more regular tetrahedral four-co-ordinate $[Hg(SC_6H_4Ph\text{-}2)_4]^{2-}$ complex. This is not unexpected as the shielding anisotropy is expected to be sensitive to the exact geometrical and electronic arrangement of the metal–ligand system, rather than to the co-ordination number alone, which is a more superficial measure of the co-ordination environment. The asymmetry parameter η for the present complex is about 0.7, and is slightly less than the values 0.8–0.9 which have been observed for strongly distorted trigonal-planar species such as $[Hg(SPh)_3]^-$.[21] This value is, however, considerably greater than those for compounds which contain only slightly distorted trigonal three-co-ordinate or linear two-co-ordinate Hg; for perfectly symmetrical structures of this type the asymmetry parameter would be zero, as it is in $[NMe_4][Hg(SPr^i)_3]$ (Table 2), but small distortions from the ideal structures result in non-zero asymmetry parameters with values up to 0.3.[21] The similarity of the asymmetry parameters for the present complex and the distorted trigonal-planar species further emphasizes the similarity in the co-ordination geometries which is also reflected in the chemical shift anisotropies, as discussed above. The isotropic chemical shift δ_{iso} is about -560 for the present complex, and is somewhat more negative than the values observed for more symmetrical tetrahedral HgS_4 environments, *e.g.* δ_{iso} -433 for $[Hg(SC_6H_4Ph\text{-}2)_4]^{2-}$ (Table 2). Again, this can be understood in terms of the observed distortion in the direction from **I** to **II** illustrated above, which changes the mercury co-ordination environment from tetrahedral to something closer to linear two-co-ordinate. The isotropic chemical shift for linear two-co-ordinate HgS_2 co-ordination is much more negative, *e.g.* δ_{iso} -1015 p for $[Hg(SC_6H_2Pr^i_3\text{-}2,4,6)_2]$ (Table 2). The decrease in the chemical shift for the present complex relative to that for $[Hg(SC_6H_4Ph\text{-}2)_4]^{2-}$ is 127 ppm, compared with a decrease of 582 ppm for $[Hg(S\text{-}C_6H_2Pr^i_3\text{-}2,4,6)_2]$. This suggests that the distortion in $[Hg_2(SPh)_6]^{2-}$ is about 20% complete, and this agrees reasonably well with the observed terminal S–Hg–S bond angle (132°) which has increased by an amount which is about 30% of the total increase of 70° (110 to 180°) required for the transition from tetrahedral to digonal co-ordination. The same kind of trend is seen in the shielding anisotropy, where the increase is 26% of the difference between the values for the compounds with nearly ideal tetrahedral and linear co-ordination environments. Thus, both the isotropic and anisotropic ^{199}Hg chemical shift parameters can be understood in terms of the distorted tetrahedral geometry which is observed in the crystal structure of the complex.

As expected, the CP MAS ^{13}C NMR spectrum is complex. Three distinct regions are observed. The methyl protons gave two signals, at δ_C 55.5 and 56.5. It is presumed that these correspond to the two non-equivalent NMe_4^+ ions in the unit cell, but that rotation of the ions probably renders the four methyls of a given ion equivalent on the NMR time-scale. The quaternary carbon signals of the phenyl groups (distinguished by a dipolar dephasing experiment) lie between δ_C 143 and 148. Most intensity lies in three peaks at δ_C 144.2, 145.1 and 147.7, and it is tempting to assign the last to the bridging SPh groups. The aromatic CH resonances lie between δ_C 121 and 132, with a prominent gap near δ_C 126. It is not clear whether 180° ring flips of the phenyl groups are rapid on the NMR time-scale. In general the ^{13}C spectrum is consistent with the structure as determined by X-ray diffraction.

Solution NMR spectroscopy

The ^{199}Hg NMR spectrum of $[NMe_4]_2[Hg_2(SPh)_6]$ in solution (0.1 mol dm^{-3} in dmso at 298 K) gave a single line at δ -401. This is closer to the value δ -341 found previously for the trigonal monomer $[Hg(SPh)_3]^-$ in $[NBu^n_4][Hg(SPh)_3]$[21,43] than that of δ -560 found in the present study for dinuclear $[Hg_2(SPh)_6]^{2-}$ in $[NMe_4]_2[Hg_2(SPh)_6]$. This implies that the structure in solution is closer to that found in the former compound in the solid state, *i.e.* monomeric. It therefore appears that $[Hg_2(SPh)_6]^{2-}$ dissociates readily in solution to give $[Hg(SPh)_3]^-$, and this view is supported by electrospray mass spectrometry studies, as discussed below.

Electrospray mass spectrometry

Electrospray mass spectrometry (ESMS) is a relatively new soft-ionization technique which has been successfully employed in the study of large biomolecules such as proteins and oligonucleotides,[46] and is being applied to an increasing extent to the characterization of charged inorganic molecules.[47] In order to investigate the relationship between the solution chemistry of mercury(II) thiolate complexes and the species detected in ESMS, we have recorded and analysed the spectrum of $[NMe_4]_2[Hg_2(SPh)_6]$ dissolved in acetonitrile–water (1 : 1 v/v), and the spectrum run at a cone voltage of 20 V is shown in Fig. 6. The most intense peak in the spectrum occurs at m/z = 529, and this can be unambiguously assigned to the $[Hg(SPh)_3]^-$ ion from its isotope splitting pattern; $[Hg_2(SPh)_6]^{2-}$ would give a pattern centred at the same m/z value, but with peaks separated by 0.5 units on the m/z scale, this being the characteristic signature of a dianion. The dimerization of anionic species in ESMS has recently been demonstrated in the case of $[Cd_2(SPh)_5]^-$, where the proportion of the associated species $[Cd_4(SPh)_{10}]^{2+}$ increased as the cone voltage in the spectrometer was reduced from 20 to 5 V.[48] However, lowering the cone voltage to 5 V in the present case resulted in no change in the isotope splitting pattern, indicating that $[Hg_2(SPh)_6]^{2-}$ is either not present in solution, or that it is very unstable with respect to dissociation into monomeric $[Hg(SPh)_3]^-$.

The solution ^{199}Hg NMR results discussed above indicate that $[Hg_2(SPh)_6]^{2-}$ readily dissociates in solution, which suggests that the absence of the dianion in the ESMS is the result of the absence of this species in solution. The other main peaks in the spectrum are assigned to SPh^- (m/z = 109) and $[Hg_2(SPh)_5]^-$ (m/z = 947). The spectrum does not change much upon reducing the cone voltage to 5 V. However, at a cone voltage of 60 V the SPh^- peak becomes predominant, while those due to $[Hg(SPh)_3]^-$ and $[Hg_2(SPh)_5]^-$ essentially disappear. This implies that the dissociation $[Hg(SPh)_3]^- \longrightarrow [Hg(SPh)_2] + SPh^-$ occurs relatively easily, and contrasts with the behaviour of $[Cd(SPh)_3]^-$ which gives a very strong peak in the spectrum at cone voltages up to 120 V.[48] This is probably due to the tendency for mercury(II) to engage in two- rather than three-co-ordination, a tendency which is not shown by cadmium(II).

Conclusion

The $[Hg_2(SPh)_6]^{2-}$ ion has been characterized in the solid state as its $[NMe_4]^+$ salt. This compound had allowed the measurement of the ^{199}Hg anisotropic NMR shielding parameters for mercury in an HgS_4 environment involving two terminal and two doubly bridging thiolate sulfur atoms. Comparison of these parameters with those previously determined for mononuclear complexes involving terminal HgS_2, HgS_3 and HgS_4 co-ordination with thiolate ligands confirms that they are very sensitive to changes in the mercury co-ordination environment. Solution ^{199}Hg NMR and electrospray mass spectra show that $[Hg_2(SPh)_6]^{2-}$ dissociates

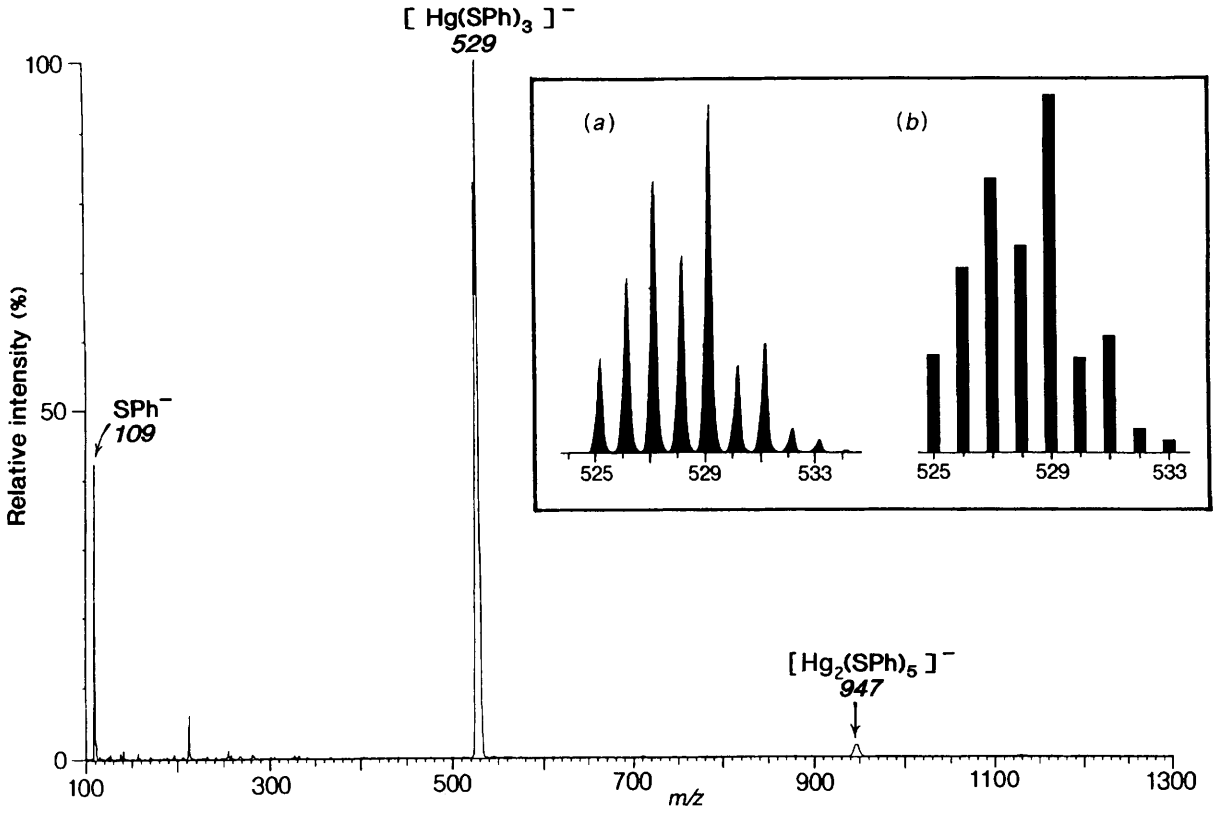

Fig. 6 Negative-ion electrospray mass spectrum of $[NMe_4]_2[Hg_2(SPh)_6]$ in acetonitrile–water (1 : 1 v/v) solution run at a cone voltage of 20 V. The inset shows (*a*) the observed and (*b*) the calculated isotope distribution patterns for the $[Hg(SPh)_3]^-$ ion

readily into $[Hg(SPh)_3]^-$ in solution, and this is consistent with evidence from the crystal structure which shows that the bridge bonding in the dimer is relatively weak.

Acknowledgements

We thank the University of Auckland Research Committee and the New Zealand Lottery Grants Board for financial support. We thank Dr. D. C. Apperley for invaluable help in operating the Varian NMR spectrometer. We acknowledge support from the EPSRC (UK) for use of the system under the Solid-state NMR Service based in Durham. One of us (S.-W. O.) is grateful to the Ministry of Education, Republic of Korea, for an award under the professors' training programme.

References

1 *Metallothionein II*, eds. J. H. R. Kägi and Y. Kojima, Birkhäuser, Basle, 1987.
2 W. F. Furey, A. H. Robbins, L. L. Clancy, D. R. Winge, B. C. Wang and C. D. Stout, *Science*, 1986, **231**, 704.
3 E. S. Gruff and S. A. Koch, *J. Am. Chem. Soc.*, 1990, **112**, 1245.
4 J. G. Wright, H.-T. Tsang, J. E. Penner-Hahn and T. V. O'Halloran, *J. Am. Chem. Soc.*, 1990, **112**, 2434.
5 S. P. Watton, J. G. Wright, F. M. MacDonnell, J. W. Bryson, M. Sabat and T. V. O'Halloran, *J. Am. Chem. Soc.*, 1990, **112**, 2824.
6 J. G. Wright, M. J. Natan, F. M. MacDonnell, D. M. Ralston and T. V. O'Halloran, *Prog. Inorg. Chem.*, 1990, **38**, 323.
7 I. G. Dance, *Polyhedron*, 1986, **5**, 1037.
8 P. J. Blower and J. R. Dilworth, *Coord. Chem. Rev.*, 1987, **76**, 121.
9 B. A. Johnson and I. M. Armitage, *Inorg. Chem.*, 1987, **26**, 3139.
10 D. C. Bradley and N. R. Kunchur, *J. Chem. Phys.*, 1964, **40**, 2258; *Can. J. Chem.*, 1965, **43**, 2786.
11 N. J. Taylor and A. J. Carty, *J. Am. Chem. Soc.*, 1977, **99**, 6143.
12 B. M. Alsaadi and M. Sandström, *Acta Chem. Scand., Ser. A*, 1982, **36**, 509.
13 H. Barrera, J. C. Bayón, P. González-Duarte, J. Sola, J. M. Viñas, J. L. Briansó, M. C. Briansó and X. Solans, *Polyhedron*, 1982, **1**, 647.
14 S. Wang and J. P. Fackler, jun., *Inorg. Chem.*, 1989, **28**, 2615.
15 E. Block, M. Brito, M. Gernon, D. McGowty, H. Kang and J. Zubieta, *Inorg. Chem.*, 1990, **29**, 3172.
16 I. Casals, P. González-Duarte and W. Clegg, *Inorg. Chim. Acta*, 1991, **184**, 167.
17 N. R. Kunchur, *Nature (London)*, 1964, **204**, 468.
18 C. Stålhandske and F. Zintl, *Acta Crystallogr., Sect. C*, 1987, **43**, 863.
19 T. Alsina, W. Clegg, K. A. Fraser and J. Sola, *J. Chem. Soc., Dalton Trans.*, 1992, 1393.
20 G. Christou, K. Folting and J. C. Huffmann, *Polyhedron*, 1984, **3**, 1247.
21 R. A. Santos, E. S. Gruff, S. A. Koch and G. S. Harbison, *J. Am. Chem. Soc.*, 1991, **113**, 469.
22 G. A. Bowmaker, I. G. Dance, B. C. Dobson and D. A. Rogers, *Aust. J. Chem*, 1984, **37**, 1607.
23 I. L. Abrahams, C. D. Garner and W. Clegg, *J. Chem. Soc., Dalton Trans.*, 1987, 1577.
24 A. D. Watson, Ch. Pulla Rao, J. R. Dorfman and R. H. Holm, *Inorg. Chem.*, 1985, **24**, 2820.
25 B. R. Hollebone and R. S. Nyholm, *J. Chem. Soc. A*, 1971, 332.
26 L. Birkenbach and K. Kellerman, *Ber. Dtsch. Chem. Ges.*, 1925, **58**, 786; 2377.
27 P. L. Goggin, P. King, D. M. McEwan, G. E. Taylor, P. Woodward and M. Sandström, *J. Chem. Soc., Dalton Trans.*, 1982, 875.
28 G. S. Harris, F. Inglis, J. McKechnie, K. K. Cheung and G. Ferguson, *Chem. Commun.*, 1967, 442.
29 J. G. Contreras, G. V. Seguel and W. Hölne, *J. Mol. Struct.*, 1980, **68**, 1.
30 D. N. Waters, E. L. Short, M. Tharwat and D. F. C. Morris, *J. Mol. Struct.*, 1973, **17**, 389; D. N. Waters, Z. Kantarci and N. N. Rahman, *J. Raman Spectrosc.*, 1978, **7**, 288.
31 R. M. Herath Banda, I. G. Dance, T. D. Bailey, D. C. Craig and M. L. Scudder, *Inorg. Chem.*, 1989, **28**, 1862.
32 A. D. Rae, RAELS, A Comprehensive Constrained Least-squares Refinement Program, University of New South Wales, 1989.
33 J. A. Ibers and W. C. Hamilton (Editors), *International Tables for X-Ray Crystallography*, Kynoch Press, Birmingham, 1974, vol. 4.
34 C. K. Johnson, ORTEP II, Report ORNL-5138, Oak Ridge National Laboratory, Oak Ridge, TN, 1976.
35 T. Bjorholm and H. J. Jakobsen, *J. Magn. Reson.*, 1989, **84**, 204.

36 J. R. Ascenso, H. Bai and R. K. Harris, unpublished work; R. K. Harris, L. H. Merwin and G. Hägele, *J. Chem. Soc., Faraday Trans. 1*, 1989, 1409.
37 J. M. Hook, P. A. W. Dean and L. C. M. van Gorkom, *Magn. Reson. Chem.*, 1995, **33**, 77.
38 M. A. Sens, N. K. Wilson, P. D. Ellis and J. D. Odom, *J. Magn. Reson.*, 1975, **19**, 323.
39 L. J. Arnold, *J. Chem. Educ.*, 1992, **69**, 811.
40 N. Ueyama, T. Sugawara, K. Sasaki, A. Nakamura, S. Yamashita, Y. Wakatsuki, H. Yamazaki and N. Yasuoka, *Inorg. Chem.*, 1988, **27**, 741.
41 J. Liesk and G. Klar, *Z. Anorg. Allg. Chem.*, 1977, **435**, 103.
42 I. G. Dance and M. Scudder, *J. Chem. Soc., Chem. Commun.*, 1995, 1039.
43 M. J. Natan, C. F. Millikan, J. G. Wright and T. V. O'Halloran, *J. Am. Chem. Soc.*, 1990, **112**, 3255.
44 M. Han, O. B. Peerson, J. W. Bryson, T. V. O'Halloran and S. O. Smith, *Inorg. Chem.*, 1995, **34**, 1187.
45 R. K. Harris and A. Sebald, *Magn. Reson. Chem.*, 1987, **25**, 1058.
46 R. D. Smith, J. A. Loo, C. G. Edmonds, C. J. Barinaga and H. R. Udseth, *Anal. Chem.*, 1990, **62**, 882.
47 T.-C. Lau, J. Wang, R. Guevremont and K. W. M. Siu, *J. Chem. Soc., Chem. Commun.*, 1995, 877; R. Arakawa, T. Matsuo, K. Nozaki, T. Ohno and M. Haga, *Inorg. Chem.*, 1995, **34**, 2464; A. M. Bond, R. Colton, Y. A. Mah and J. C. Traeger, *Inorg. Chem.*, 1994, **33**, 2548.
48 T. Løver, G. A. Bowmaker, W. Henderson and R. P. Cooney, *J. Chem. Soc., Chem. Commun.*, 1996, 683

Received 7th December 1995; *Paper* 5/07996I